Synthesis of Molybdenum Nanowires with Millimeter-Scale Lengths Using Electrochemical Step Edge Decoration

M. P. Zach, K. Inazu, K. H. Ng, J. C. Hemminger, and R. M. Penner*

Department of Chemistry, University of California, Irvine, California 92697-2025

Received March 7, 2002. Revised Manuscript Received May 10, 2002

Molybdenum (Mo^0) nanowires with diameters ranging from 13 nm to 1 μm and having lengths of up to 500 μm have been synthesized by a two-step process involving the electrodeposition of molybdenum dioxide (MoO_2) on a highly oriented pyrolytic graphite (HOPG) surface followed by reduction of the MoO_2 nanowires at 500 °C to form molybdenum metal. MoO_2 nanowires were electrodeposited reductively from an alkaline MoO_4^{2-} solution using a low overpotential of $<|200$ mV$|$. Under these conditions, the nucleation of MoO_2 occurred selectively at step edges present on the HOPG surface, and a high linear density (>30 μm^{-1}) of MoO_2 nuclei was formed along each step edge on the graphite surface. With continued growth, MoO_2 nuclei that were 10−15 nm in diameter coalesced with adjacent nuclei along the step edge to form continuous nanowires having approximately this same diameter. Longer deposition times, t_{dep}, produced smooth MoO_2 nanowires with diameters proportional to $t_{dep}^{1/2}$. These nanowires had a uniform diameter and a smooth surface, and the nanowire-to-nanowire variation in diameter was 10−30%. In contrast to nanowires of MoO_2, which were brittle and subject to breakage, molybdenum metal (Mo^0) nanowires were resilient and resistant to breakage. Arrays of Mo^0 nanowires could be embedded in a polymer film and lifted off the graphite surface. In humid air (≈55% relative humidity) at room temperature, the resistivity of Mo^0 nanowires increased by 10% h^{-1} as an insulating surface oxide of MoO_3 formed.

I. Introduction

Interest in nanowires derives in part from the intriguing physics of these structures: quantum effects are manifested in the electronic,[1−7] magnetic,[4,8−13] and mechanical[14−17] properties of metal nanowires. Nanowire research is also motivated by the likelihood that nanometer-scale interconnects will be required in future generations of nanometer-scale electronics. Finally, nanowires are providing new opportunities for the design of small, selective, and fast chemical sensors.[18−22]

The word "nanowire" has appeared in the titles of over 700 journal articles as of this writing, with approximately 50% of these appearing in 2000 and 2001. A review of this literature reveals that the definition adopted for the word nanowire is broad and variable. For example, fully a third of these papers report fundamental studies of transport in nanoconstrictions, nanowires that have nanometer-scale length (<50 nm) as well as diameter. At least 13 methods for synthesizing nanowires have been described in this literature, but of these we have found just three that permit the preparation of free-standing metal nanowires with

* To whom correspondence should be addressed. E-mail: rmpenner@uci.edu.

(1) Escapa, L.; Garcia, N. *Appl. Phys. Lett.* **1990**, *56*, 901.
(2) CostaKramer, J. L.; Garcia, N.; Olin, H. *Phys. Rev. Lett.* **1997**, *78*, 4990.
(3) Zhang, Z. B.; Sun, X. Z.; Dresselhaus, M. S.; Ying, J. Y.; Heremans, J. *Phys. Rev. B* **2000**, *61*, 4850.
(4) Zhang, Z. B.; Sun, X. Z.; Dresselhaus, M. S.; Ying, J. Y.; Heremans, J. P. *Appl. Phys. Lett.* **1998**, *73*, 1589.
(5) Pascual, J. I.; Mendez, J.; Gomezherrero, J.; Baro, A. M.; Garcia, N.; Binh, V. T. *Phys. Rev. Lett.* **1993**, *71*, 1852.
(6) Pascual, J. I.; Mendez, J.; Gomezherrero, J.; Baro, A. M.; Garcia, N.; Landman, U.; Leudtke, W. D.; Bogachek, E. N.; Cheng, H. P. *J. Vac. Sci. Technol. B* **1995**, *13*, 1280.
(7) Pascual, J. I.; Mendez, J.; Gomezherrero, J.; Baro, A. M.; Garcia, N.; Landman, U.; Luedtke, W. D.; Bogachek, E. N.; Cheng, H. P. *Science* **1995**, *267*, 1793.
(8) Heremans, J.; Thrush, C. M.; Zhang, Z.; Sun, X.; Dresselhaus, M. S.; Ying, J. Y.; Morelli, D. T. *Phys. Rev. B: Condens. Matter Mater. Phys.* **1998**, *58*, 10091.
(9) Bogachek, E. N.; Scherbakov, A. G.; Landman, U. *Phys. Rev. B: Condens. Matter Mater. Phys.* **1996**, *53*, 13246.
(10) Bogachek, E. N.; Scherbakov, A. G.; Landman, U. *Phys. Rev. B: Condens. Matter Mater. Phys.* **1997**, *56*, 14917.
(11) Liu, K.; Chien, C. L.; Searson, P. C.; Kui, Y. Z. *Appl. Phys. Lett.* **1998**, *73*, 1436.
(12) Liu, K.; Nagodawithana, K.; Searson, P. C.; Chien, C. L. *Phys. Rev. B: Condens. Matter Mater. Phys.* **1995**, *51*, 7381.
(13) Liu, K.; Chien, C. L.; Searson, P. C. *Phys. Rev. B: Condens. Matter Mater. Phys.* **1998**, *58*, R14681.
(14) Landman, U.; Luedtke, W. D.; Salisbury, B. E.; Whetten, R. L. *Phys. Rev. Lett.* **1996**, *77*, 1362.
(15) Yannouleas, C.; Landman, U. *J. Phys. Chem. B* **1997**, *101*, 5780.
(16) Ikeda, H.; Qi, Y.; Cagin, T.; Samwer, K.; Johnson, W. L.; Goddard, W. A. *Phys. Rev. Lett.* **1999**, *82*, 2900.
(17) Blom, S.; Olin, H.; CostaKramer, J. L.; Garcia, N.; Jonson, M.; Serena, P. A.; Shekhter, R. I. *Phys. Rev. B: Condens. Matter Mater. Phys.* **1998**, *57*, 8830.
(18) Bogozi, A.; Lam, O.; He, H. X.; Li, C. Z.; Tao, N. J.; Nagahara, L. A.; Amlani, I.; Tsui, R. *J. Am. Chem. Soc.* **2001**, *123*, 4585.
(19) Li, C. Z.; He, H. X.; Tao, N. J. *Appl. Phys. Lett.* **2000**, *77*, 3995.
(20) Li, C. Z.; He, H. X.; Bogozi, A.; Bunch, J. S.; Tao, N. J. *Appl. Phys. Lett.* **2000**, *76*, 1333.
(21) Cui, Y.; Wei, Q. Q.; Park, H. K.; Lieber, C. M. *Science* **2001**, *293*, 1289.
(22) Favier, F.; Walter, E. C.; Zach, M. P.; Benter, T.; Penner, R. M. *Science* **2001**, *293*, 2227.

10.1021/cm020249a CCC: $22.00
Published on Web 06/22/2002

lengths of more than a few microns: (1) template synthesis,[12,23−32] (2) fullerene encapsulation,[33−38] and (3) bulk chemical reduction in micellar solutions.[39−41]

We have recently reported[42] a new method, called electrochemical step edge decoration (ESED), by which molybdenum nanowires of 100 μm or more in length may be prepared. These nanowires can have any diameter in the range from 10 nm to 1 μm, are hemicylindrical in cross section, and are free-standing. As shown in Scheme 1, molybdenum nanowire growth is a two-step process: First, nanowires composed of an amorphous metal oxide (e.g., MoO_2) are selectively electrodeposited from a soluble precursor (e.g., MoO_4^{2-}) at the step edges on a graphite surface. Then, these resistive oxide nanowires are reduced in gaseous hydrogen at elevated temperature to yield nanowires of the parent metal (e.g., Mo^0) that have a much lower electrical resistivity. In contrast to previous work in which the step decoration method has been used to prepare "nanowires" with monatomic thickness on silicon and other substrates,[43−52] nanowires produced by electrodeposition are three-dimensional, are highly dimensionally uniform, and are removable from the graphite surfaces on which they are formed.[42] This combination of attributes is, we believe, unique to metal nanowires prepared by ESED. In this paper, we provide a detailed description of this method, and we disclose our results relating to the chemical and electrical properties of the molybdenum nanowires produced by ESED.

Scheme 1. Depiction of the Method of Preparation for Molybdenum Nanowires Using ESED on a Graphite Surface

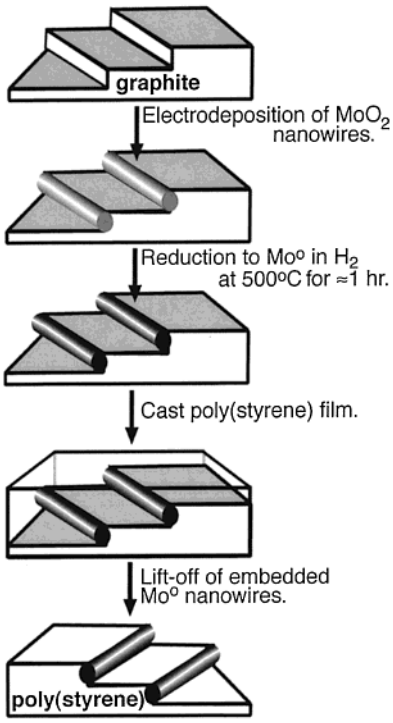

II. Experimental Section

Molybdenum Dioxide Electrodeposition. Molybdenum dioxide nanowires were electrodeposited from aqueous plating solutions containing Na_2MoO_4 (0.1−10 mM, 98+% anhydrous; Aldrich), 1.0 M NaCl (Fischer-certified ACS grade), and 1.0 M NH_4Cl (J. T. Baker) adjusted to pH 8.5 using aqueous ammonium hydroxide (Fischer ACS grade) and purged with N_2. These solutions were prepared using Barnsted Nanopure water (σ > 17 MΩ cm^{-1}). A basal plane oriented, 12 × 12 × 1 mm piece of highly oriented pyrolytic graphite (HOPG) was employed as the working electrode in a three-electrode cell with a large-area platinum counter electrode and a saturated calomel reference electrode (SCE). In experiments involving either cyclic voltammetry or the measurement of plating current transients, just one (0001) surface of these HOPG pieces was exposed to the plating solution; the edges and backside of the piece were masked using Apiezon W wax. Nanowire growth experiments, however, were generally carried out by exposing both edges and basal plane surfaces of the HOPG to the plating solution. In these experiments, the HOPG

(23) Brumlik, C. J.; Martin, C. R. *J. Am. Chem. Soc.* **1991**, *113*, 3174.
(24) Oskam, G.; Long, J. G.; Natarajan, A.; Searson, P. C. *J. Phys. E: Appl. Phys.* **1998**, *31*, 1927.
(25) Foss, C. A.; Tierney, M. J.; Martin, C. R. *J. Phys. Chem.* **1992**, *96*, 9001.
(26) Martin, C. R. *Adv. Mater.* **1991**, *3*, 457.
(27) Searson, P. C.; Cammarata, R. C.; Chien, C. L. *J. Electron. Mater.* **1995**, *24*, 955.
(28) Whitney, T. M.; Jiang, J. S.; Searson, P. C.; Chien, C. L. *Science* **1993**, *261*, 1316.
(29) Foss, C. A.; Tierney, M. J.; Martin, C. R. *J. Phys. Chem.* **1992**, *96*, 9001.
(30) Brumlik, C. J.; Menon, V. P.; Martin, C. R. *J. Mater. Res.* **1994**, *9*, 1174.
(31) Cepak, V. M.; Martin, C. R. *J. Phys. Chem. B* **1998**, *102*, 9985.
(32) Preston, C. K.; Moskovits, M. *J. Phys. Chem.* **1993**, *97*, 8495.
(33) Hsu, W. K.; Terrones, M.; Terrones, H.; Grobert, N.; Kirkland, A. I.; Hare, J. P.; Prassides, K.; Townsend, P. D.; Kroto, H. W.; Walton, D. R. M. *Chem. Phys. Lett.* **1998**, *284*, 177.
(34) Terrones, M.; Hsu, W. K.; Schilder, A.; Terrones, H.; Grobert, N.; Hare, J. P.; Zhu, Y. Q.; Schwoerer, M.; Prassides, K.; Kroto, H. W.; Walton, D. R. M. *Appl. Phys. A: Mater. Sci. Process.* **1998**, *66*, 307.
(35) Terrones, M.; Grobert, N.; Hsu, W. K.; Zhu, Y. Q.; Hu, W. B.; Terrones, H.; Hare, J. P.; Kroto, H. W.; Walton, D. R. M. *MRS Bull.* **1999**, *24*, 43.
(36) Hsu, W. K.; Trasobares, S.; Terrones, H.; Terrones, M.; Grobert, N.; Zhu, Y. Q.; Li, W. Z.; Escudero, R.; Hare, J. P.; Kroto, H. W.; Walton, D. R. M. *Chem. Mater.* **1999**, *11*, 1747.
(37) Guerretpiecourt, C.; Lebouar, Y.; Loiseau, A.; Pascard, H. *Nature* **1994**, *372*, 761.
(38) Setlur, A. A.; Lauerhaus, J. M.; Dai, J.-Y.; Chang, R. P. H. *Appl. Phys. Lett.* **1996**, *69*, 345.
(39) Jana, N. R.; Gearheart, L.; Murphy, C. J. *Chem. Commun.* **2001**, 617.
(40) Jana, N. R.; Gearheart, L.; Murphy, C. J. *J. Phys. Chem. B* **2001**, *105*, 4065.
(41) Jana, N. R.; Gearheart, L.; Murphy, C. J. *Adv. Mater.* **2001**, *13*, 1389.
(42) Zach, M. P.; Ng, K. H.; Penner, R. M. *Science* **2000**, *290*, 2120.
(43) Petrovykh, D. Y.; Himpsel, F. J.; Jung, T. *Surf. Sci.* **1998**, *407*, 189.
(44) Morin, S.; Lachenwitzer, A.; Magnussen, O. M.; Behm, R. J. *Phys. Rev. Lett.* **1999**, *83*, 5066.
(45) Abd El Meguid, E. A.; Berenz, P.; Baltruschat, H. *J. Electroanal. Chem.* **1999**, *467*, 50.
(46) Himpsel, F. J.; Jung, T.; Kirakosian, A.; Lin, J. L.; Petrovykh, D. Y.; Rauscher, H.; Viernow, J. *MRS Bull.* **1999**, *24*, 20.
(47) Dekoster, J.; Degroote, B.; Pattyn, H.; Langouche, G.; Vantomme, A.; Degroote, S. *Appl. Phys. Lett.* **1999**, *75*, 938.
(48) Kawakami, R. K.; Bowen, M. O.; Choi, H. J.; Escorcia-Aparicio, E. J.; Qiu, Z. Q. *J. Appl. Phys.* **1999**, *85*, 4955.
(49) Blanc, M.; Kuhnke, K.; Marsico, V.; Kern, K. *Surf. Sci.* **1998**, *414*, L964.
(50) Gambardella, P.; Blanc, M.; Brune, H.; Kuhnke, K.; Kern, K. *Phys. Rev. B* **2000**, *61*, 2254.
(51) Dallmeyer, A.; Carbone, C.; Eberhardt, W.; Pampuch, C.; Rader, O.; Gudat, W.; Gambardella, P.; Kern, K. *Phys. Rev. B* **2000**, *61*, R5133.
(52) Noll, J. D.; Nicholson, M. A.; VanPatten, P. G.; Chung, C. W.; Myrick, M. L. *J. Electrochem. Soc.* **1998**, *145*, 3320.

working electrode was simply suspended in the plating solution using stainless steel forceps. Nanowire electrodeposition and cyclic voltammetry were both performed using a computer-controlled EG&G 273A potentiostat.

Reduction of MoO_2 to Molybdenum and Removal from HOPG. Nanowires prepared using the procedure described above were composed primarily of molybdenum dioxide (see the discussion below). The reduction of MoO_2 nanowires to molybdenum metal was effected by heating the graphite working electrode in a tube furnace at 500−650 °C under an atmosphere of pure hydrogen or a 10% hydrogen/90% nitrogen mixture for 1−3 h depending on the wire diameter. The reduced molybdenum nanowire was lifted off of the HOPG surface by casting a polystyrene film using 1 drop of a 20 wt % polystyrene (from a Styrofoam cup) solution in acetone (Fischer ACS grade). After drying in air, the resulting film with embedded nanowires was peeled off the graphite surface using forceps. Free-standing molybdenum nanowires could be released from the polystyrene film by stretching this film by a few percent.

Assessment of Nanowire Environmental Stability. The stability of molybdenum nanowires was evaluated by monitoring the resistance of arrays of 10−100 nanowires connected electrically in parallel. These nanowire arrays were prepared by first lifting nanowires off the graphite, excising a 1 × 1 mm section of this polymer film encompassing a nanowire array, and then attaching this nanowire array on the edge of a copper-cladded circuit board (total size 1 × 1 cm) using a commercial cyanoacrylate adhesive (HotStuff Special T Satellite City, Simi, CA). Electrical contacts between the two ends of the nanowire arrays and the two copper surfaces of the circuit board were deposited by first masking the centers of the nanowire array with a flattened copper wire with a width of 60−120 μm and then sputter-depositing a 100−200 nm gold layer. After removal of the copper wire, excess gold was removed from the device using a razor blade.

X-ray Photoelectron Spectroscopy. X-ray photoelectron spectroscopy (XPS) was carried out using an ESCALAB MKII photoelectron spectrometer (VG Scientific). The ESCALAB MKII is a multitechnique surface analysis instrument based on an ultrahigh-vacuum (UHV) system consisting of three separately pumped, interconnected chambers (sample preparation, fast sample entry, and spectroscopy). The fast entry chamber allowed rapid sample transfer from air to UHV pressures (base pressures during XPS analysis were in the low- to mid-10^{-10} Torr range). The XPS experiments were performed in the spectroscopy chamber using a standard Mg anode X-ray source (and the Mg Kα X-ray line at 1253.6 eV) and a 150 mm hemispherical electron energy analyzer. The spectra presented here were obtained using an analyzer pass energy of 20 eV. Under these conditions the spectrometer energy resolution was ∼0.8 eV. Samples were prepared by supporting the graphite surface, upon which the nanowires were prepared, on a copper sample holder using conductive colloidal silver paste (Ted Pella).

Electron Microscopy. Scanning electron microscopy (SEM) was carried out on uncoated samples using a Philips FEG-30XL microscope equipped with EDAX elemental analysis capabilities. Transmission electron microscopy (TEM) was carried out using a Philips CM-20. HOPG flakes with attached nanowires were transferred to uncoated copper grids (uncoated copper; Ted Pella) for analysis using TEM. These flakes were obtained by mechanically scraping the HOPG surface with the grid.

III. Results and Discussion

III.A. Nanowire Electrodeposition. ESED relies on the fact that a nucleation barrier exists for the formation of a new phase on a clean graphite electrode. This barrier is slightly lower at steps than at terraces, and this energetic disparity for nucleation can be exploited by selecting a deposition potential near the threshold for nucleation at step edges. This threshold potential is readily located by examining the cyclic voltammetry of a graphite surface in the deposition solution of interest. In the case of MoO_2 deposition, this solution contains the precursor MoO_4^{2-}, and deposition involves its reduction:

$$MoO_4^{2-} + 2H_2O + 2e^- \rightarrow MoO_2 + 4OH^-$$

The cyclic voltammetry of a graphite electrode in this solution is shown in Figure 1A. As the potential is scanned negatively from +0.1 to −1.25 V vs SCE, two reductions are observed: An onset for the MoO_2 deposition is seen at approximately −0.60 V, and an onset for hydrogen evolution is observed at −1.10 V. In this solution, MoO_2 can be electrodeposited at any potential negative of −0.60 V; however, the selectivity of nucleation, and therefore the distribution of MoO_2, on the graphite surface changes dramatically as the deposition overpotential is increased.

We have investigated the growth of MoO_2 as a function of the applied voltage for six voltages in the range from −0.70 to −2.2 V vs SCE. Electrode surfaces were imaged by SEM after MoO_2 was electrodeposited for 256 s (1024 s at −0.7 V). Representative images of these surfaces are shown in Figure 1. At the most positive potentials in this series (−0.70 and −0.85 V), MoO_2 nucleation occurs with a high degree of selectivity at step edges. At −0.70 V (Figure 1C), we find MoO_2 located almost exclusively along step edges on the graphite surface. At 1024 s, the nucleation of MoO_2 along these step edges is incomplete and micron-length nanowires with diameters of 10−20 nm are observed. An electrodeposition for 256 s at −0.85 V (Figure 1D) produces continuous MoO_2 nanowires of 140 nm in diameter. At this potential, MoO_2 particles are also seen on terraces, but the number density of these particles is less than 1 μm^{-2}. As the deposition potential is decreased to −1.10 V (Figure 1F), an increasing number of MoO_2 particles are observed on terraces, and after 256 s, both particles and nanowires are seen on the surface. At still more negative potentials, hydrogen evolution and MoO_2 deposition occur concurrently and dramatically higher deposition currents are seen (Figure 1B). The preponderance of particles relative to nanowires increases until, at −2.2 V, MoO_2 wires are not observed at all, even at step edges on the graphite surface. Instead, MoO_2 particles that are narrowly distributed in diameter are seen both at steps and on

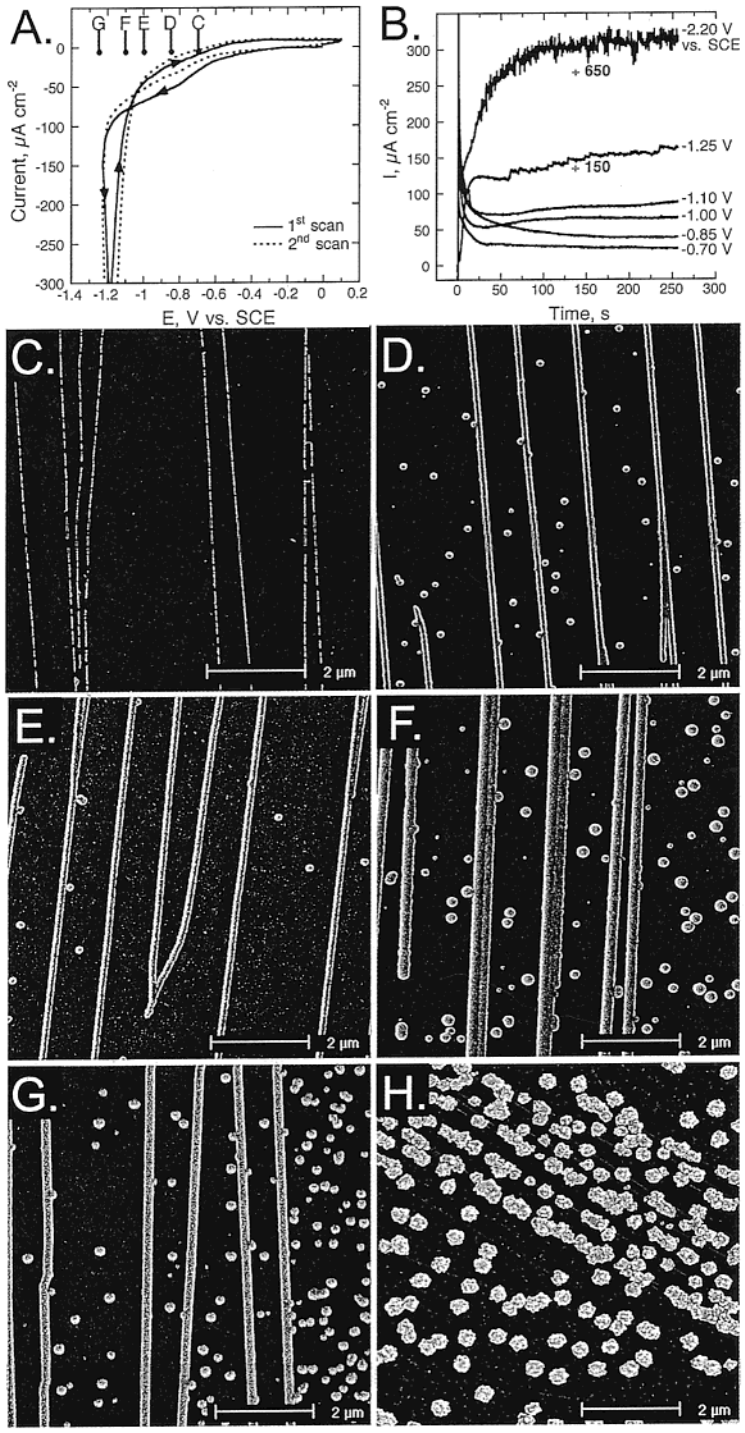

Figure 1. (A) Cyclic voltammogram at 20 mV s^{-1} for an HOPG working electrode in an aqueous plating solution containing 1 mM Na_2MoO_4, 1.0 M NaCl, and 1.0 M NH_4Cl and adjusted to pH = 8.5 with the addition of aqueous NH_3. The letters refer to the potentials used for making samples shown in the SEM images of parts C−H. (B) Current versus time for the electrodeposition of MoO_2 from the plating solution described in part A. Shown are current versus time transients for a range of different potentials, the same potentials for which SEMs are shown in parts C−H. (C−H) SEM images of graphite surfaces after the electrodeposition of MoO_2 for 256 s (or 1024 s in part C only). The plating solution in these experiments was 7 mM Na_2MoO_4, 1.0 M NaCl, and 1.0 M NH_4Cl at pH = 8.5. The deposition potential becomes progressively more negative in these six experiments as follows: −0.70 V vs SCE (C), −0.85 V (D), −0.95 V (E), −1.1 V (F), −1.25V (G), and −2.2 V (H). For plating potentials more positive than −0.80 V (see part C), the MoO_2 deposition is localized to the step edges, but it is very slow and yields discontinuous wires. At slightly more negative potentials of −0.80 to −1.1 V, the rate of MoO_2 electrodeposition is faster, but an increasing number of MoO_2 nuclei are observed on flat terraces, away from step edges on the surface. At −1.25 V, the rate of H_2 coevolution is appreciable and discontinuous MoO_2 wires are observed together with MoO_2 particles on terraces. At −2.20 V, MoO_2 wires are broken up by vigorous hydrogen evolution and particles moving across the surface. The particles appear granular and seem to be composed of smaller fragments of deposited wires and particles.

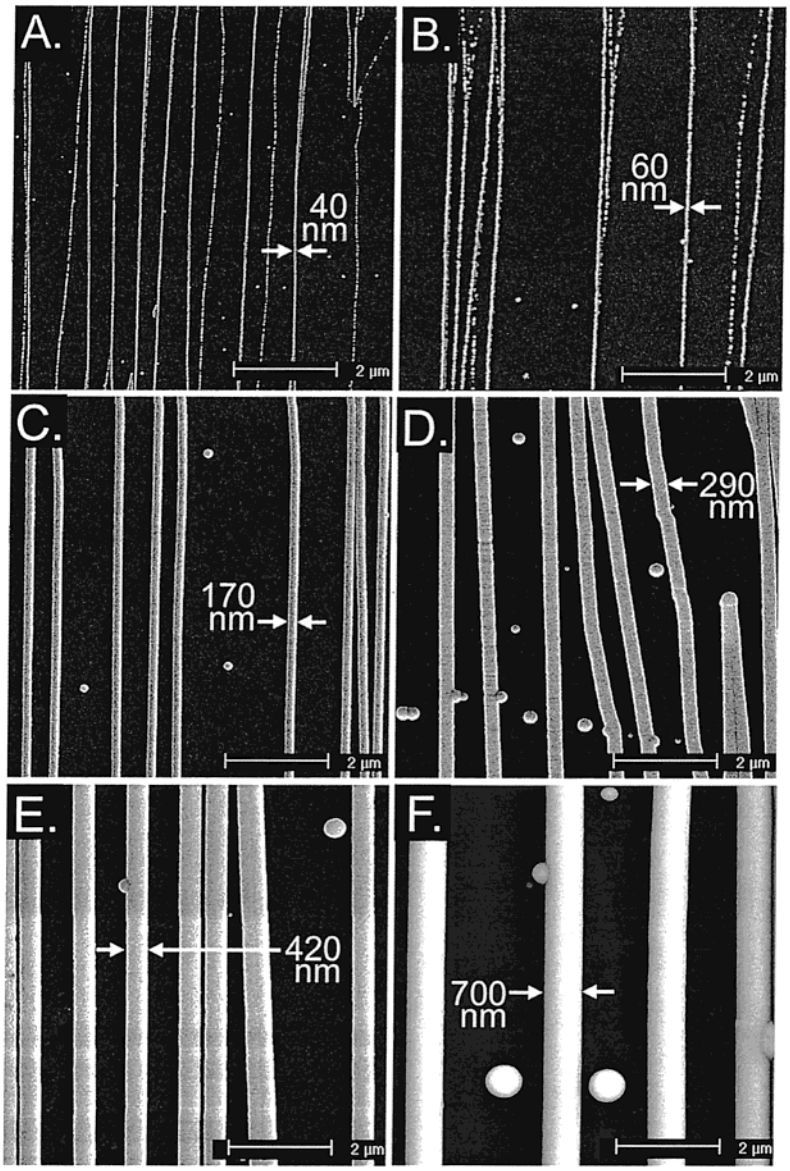

Figure 2. MoO_2 nanowires of various diameters prepared by varying the growth time as follows: 8 s (A), 16 s (B), 32 s (C), 64 s (D), 128 s (E), and 256 s (F). All wires shown here were prepared at −0.95 V vs SCE from a solution containing 7.0 mM MoO_4^{2-}, 1.0 M NaCl, and 1.0 M NH_4Cl.

terraces. We have recently demonstrated[53] that, under conditions of "hydrogen coevolution" similar to these, extremely uniform nanocrystalline nickel particles can be obtained. The key point is that, at deposition potentials in the range from −0.70 to −0.85 V, the electrodeposition of MoO_2 occurs with almost perfect site selectivity at step edges. Moreover, even though the rate of electrodeposition at these potentials is slow, the nucleation density along step edges is large ($>20\ \mu m^{-1}$) and hemispherical MoO_2 located next to one another on a step rapidly coalesce to form continuous nanowires that are many microns in length. We find that this "coalescence point" coincides with a nanowire diameter of approximately 10−15 nm.

III.B. Nanowire Characterization. As shown in Figure 1B, for potentials in the range from −0.70 to −0.85 V, the deposition current density decreases for 30−50 s from more than 100 $\mu A\ cm^{-2}$ to a time-invariant value of 20−50 $\mu A\ cm^{-2}$. If this steady-state current is associated purely with the deposition of hemicylindrical nanowires, the radius of these structures, $r(t)$, is predicted to increase according to[42]

$$r(t) = \sqrt{\frac{2 i_{dep} t_{dep} V_m}{\pi n F l}} \qquad (1)$$

where i_{dep} is the deposition current density, t_{dep} is the deposition duration, V_m is the molar volume of the deposited material (19.8 $cm^3\ mol^{-1}$ for MoO_2), n is the number of electrons transferred for the deposition of each MoO_2 unit, and l is the total length of the nanowires on the graphite surface.

The radius ∝ time$^{1/2}$ functionality predicted by eq 1 is readily confirmed by experiment. Figure 2 shows SEMs of MoO_2 nanowires prepared at −0.85 V from a 1.0 mM MoO_4^{2-} solution using six values for t_{dep} ranging from 8 to 256 s. Nanowires varying in diameter from 40 to 700 nm are obtained. These growth conditions support the preparation of MoO_2 nanowires for which the diameter uniformity, both intrawire and interwire,

(53) Zach, M. P.; Penner, R. M. *Adv. Mater.* **2000**, *12*, 878.

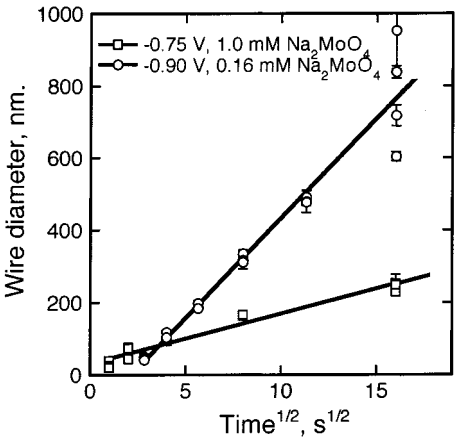

Figure 3. Plot of the MoO_2 nanowire diameter as a function of the square root of the deposition time. Linear plats, in accordance with eq 1, are obtained for two different sets of growth conditions (MoO_4^{2-} concentration and deposition potential, as indicated). Figure 1B shows the current reaching steady state; therefore, the volume of MoO_2 deposited per unit time is constant. The diameter is proportional to the cubed root of volume for a three-dimensional object that grows in all directions. Because the length of the nanowires is fixed by the length of the step edges at the beginning of the experiment, the dimension of length is a constant; thus, the volume is dependent only on two dimensions. Scatter in the diameters of the larger wires is more pronounced due to wires merging with particles and merging with other wires due to consumption of the entire width of terraces between step edges.

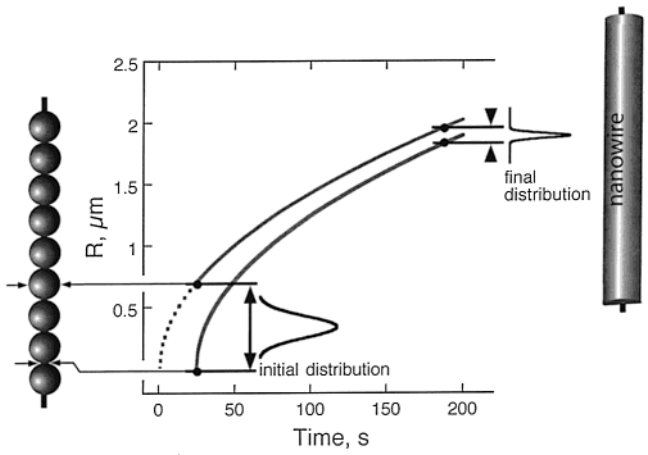

Figure 4. Schematic diagram depicting the effect of the $r \propto t^{1/2}$ growth law (eq 1) on the smoothness of a nanowire. The rate of radius growth, dr/dt, is inversely proportional to the nanowire radius. This means that constrictions along the axis of a rough nanowire are predicted to increase in radius faster than bulges on the same wire. The net effect, obtained after a period of constant current growth, is a smoothing of the nanowire surface. This explanation also accounts for the narrow size dispersion for nanowires obtained in the growth experiments described here.

is excellent. In Figure 3 we plot the nanowire diameter as a function of $t_{dep}^{1/2}$ for two sets of growth experiments involving different MoO_4^{2-} concentrations and growth potentials. The linear dependence of both plots in accordance with eq 1 is apparent. Thus, MoO_2 nanowires of a predetermined diameter can readily be obtained once the slope of the wire diameter vs $t_{dep}^{1/2}$ plot is known. It should be noted, however, that this slope depends on l, the total length of nanowires per unit area of the surface, and therefore on the step density, which varies substantially depending on the quality and source of the graphite itself.

The SEMs of Figure 2 show that MoO_2 nanowires possessed a high degree of uniformity. How is this uniformity produced during nanowire growth? The growth of nanowires occurs in three phases involving the formation of hemispherical MoO_2 nuclei along the step edge (phase 1), the growth of these nuclei to the point where a continuous, but rough nanowire exists along the step (phase 2), and subsequent growth of this nanowire (phase 3). For MoO_2, nanowires that are continuous for several microns have a diameter of 15−20 nm. At the beginning of phase 3 growth, it is obvious that these 15−20 nm nanowires become smoother as a function of growth time and that the smooth surface of the nanowire is maintained as its radius increases with continued growth up to the micron scale. This is a striking aspect of nanowire growth because it is far more common to observe dendritic growth, characterized by disordering and roughening of an electrodeposit, during electrodeposition. Why is nanowire electrodeposition a "convergent growth" process? Our hypothesis is that the growth law of eq 1 plays the central role. Equation 1 is identical, in the dependence of radius on the square root of time, with the growth law observed for spherical colloid particles precipitating from solution under conditions of diffusion control.[54,55] In that case, because dr/d$t \propto t^{-1/2}$, small particles (those that have grown for a short time) grow faster than large particles (those that have grown for longer times) and a distribution of particles of different sizes becomes more size similar as the growth time increases and the mean diameter of the particles increases. As shown in Figure 4, the same analysis predicts that, in the case of "rough" nanowires, constrictions in the nanowire grow faster than bulges and nanowires become smoother as a function of time. This convergent growth behavior is an important consequence of electrochemical nanowire growth.

We have made reference repeatedly to the electrodeposition of MoO_2; however, MoO_3, an insulating oxide, can also be electrodeposited from MoO_4^{2-}-containing solutions. The Pourbaix diagram for molybdenum, shown in Figure 5, reveals that, at pH = 8.5, an extremely narrow range of potentials (≈50 mV) exists near −0.5 V vs SCE within which MoO_2 is thermodynamically stable. Our depositions were performed at potentials several hundred millivolts negative of this "window" and within the Mo metal region, as shown. However, electrodeposited molybdenum metal should react promptly with water to produce MoO_2 and H_2 gas at this pH. To identify the deposited material, we analyzed freshly deposited nanowires using XPS. A spectrum of the Mo 3d region is shown in Figure 6A and Table 1. The energy of the Mo $3d_{5/2}$ photoelectrons is 229.8 eV, which compares with literature values for MoO_2 and MoO_3 of 229.2 and 232.7 eV, respectively. We conclude that the deposited material is predominantly MoO_2.

A distinguishing characteristic of the MoO_2 nanowires prepared by ESED is their length. A low-magnification SEM image of a graphite surface following a nanowire

(54) Reetz, M. T.; Helbig, W. *J. Am. Chem. Soc.* **1994**, *116*, 7401.
(55) Sugimoto, T. *Adv. Colloid Interface Sci.* **1987**, *28*, 65.

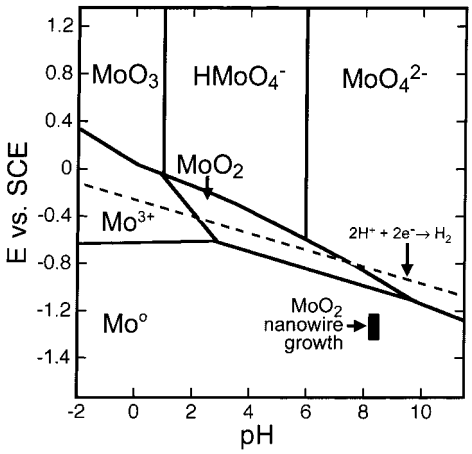

Figure 5. Pourbaix diagram for the molybdate system. This diagram shows the thermodynamically stable form of molybdenum in contact with an aqueous solution containing 1.0 mM molybdenum in the form of MoO_4^{2-} or $HMoO_4^-$, as a function of the applied potential and the pH. The black rectangle shows the region of this parameter space in which MoO_2 nanowires were obtained in this study. This rectangle is located in a region of phase space in which molybdenum metal is stable. However, this stability applies only to molybdenum metal that is maintained at the potentials indicated along the vertical axis. Upon release of the electrode surface to the open circuit, such as at the conclusion of a nanowire growth experiment, the diagram shows that it is thermodynamically favorable for Mo^0 to spontaneously oxidize to MoO_2 with the coevolution of hydrogen. Source: In *Atlas of Electrochemical Equilibria in Aqueous Solutions*; Franklin, J., Translator; Marcel Porbaix, NACE International Cebelcor: Houston, TX, 1974.

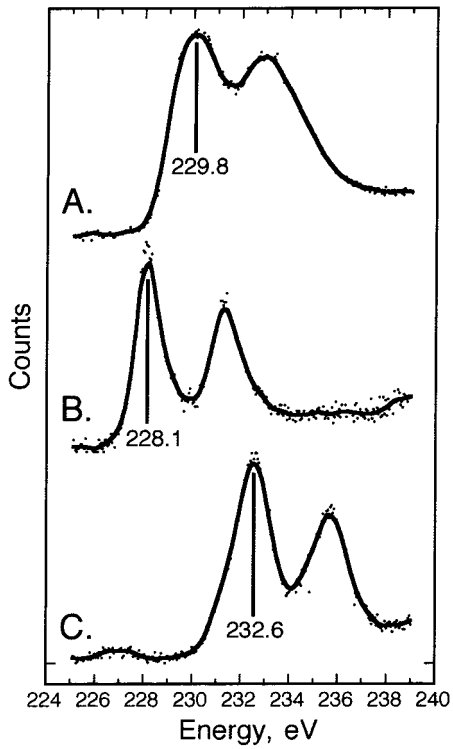

Figure 6. XPS (Mo 3d) of graphite surfaces decorated with electrodeposited nanowires. All three samples were deposited for 256 s from a solution containing 2.6 mM MoO_4^{2-} (1 M NaCl and 1 M NH_4Cl, at pH = 8.0−8.5) and consisted of nanowires approximately 400 nm in diameter. The binding energy of the Mo $3d_{5/2}$ peak is indicated for each spectrum. (A) Immediately following electrodeposition, a Mo $3d_{5/2}$ binding energy consistent with MoO_2 is observed. (B) After reduction of freshly deposited nanowires in hydrogen at 650 °C for 3 h, a Mo $3d_{5/2}$ binding energy characteristic of molybdenum metal is seen. (C) After exposure to a laboratory air ambient for approximately 5 days.

Table 1. Summary of XPS Analyses

sample	Mo $3d_{5/2}$ binding energy,[a] eV
as deposited	229.8
hydrogen reduced	228.1
air oxidized	232.6
sample	**lit. values,[b] eV**
Mo	228.0
MoO_2	229.2
MoO_3	232.7

[a] Binding energy charge compensation was done using the binding energy of 284.25 eV for the C 1s peak from HOPG. [b] Source: Moulder, J. F.; Stickle, W. F.; Sobol, P. E.; Bomben, K. D. In *Handbook of X-ray Photoelectron Spectroscopy*; Chastain, J., Ed.; Perkin-Elmer Corp.: Eden Prairie, MN, 1992; pp 112 and 113.

growth experiment is shown in Figure 7. This image shows many nanowires with lengths exceeding 200 μm or 0.2 mm. This method is the only one of which we are aware that permits the preparation of nanowires of these lengths. In general, these nanowires are aligned parallel with one another because this is the habit for step edges on the surface. With some effort, SEM images of nanowires on curved graphite surfaces can be obtained. One such image, shown in Figure 8, provides verification of the hemicylindrical shape of electrodeposited MoO_2 nanowires.

Low-magnification SEM images, like that shown in Figure 7, do not provide information on the MoO_2 nanowire uniformity. For this purpose, high-magnification images must be assembled and analyzed. The results of one such analysis, involving more than 50 SEM images, are shown in Figures 9 and 10. Here the diameter of a particular nanowire, 147 μm in length, was measured 3500 times along its axis. Histograms of the diameter measurements for three 15 μm segments of the nanowire are shown. The mean diameter varies from 113 nm in the center to 137 nm on the rightmost end, a variation of ≈20%. Within the three 15 μm segments, we calculate a relative standard deviation of the wire diameter of 10−28%. This high degree of uniformity is the result, we believe, of convergent nanowire growth resulting from the growth law of eq 1.

From an applications perspective, the many attributes of MoO_2 nanowires are overshadowed by one problem: These nanowires are extremely brittle and prone to breakage. We have not been successful in our attempts to separate these structures intact from the graphite electrode surface. However, MoO_2 is readily reduced using hydrogen at 500 °C to molybdenum metal, which is resilient and much more conductive than MoO_2. At 500 °C, this reduction requires approximately 1 h for nanowires up to 300 nm in diameter. Because the molar volume of Mo^0 is 9.4 mol cm^{-3} and that of MoO_2 is 19.8 mol cm^{-3}, nanowires shrink appreciably during this reduction process. In fact, the degree of shrinkage is 19−25% in both the nanowire length and diameter. The shrinkage in diameter is large enough to be seen in scanning electron micrographs of electrodeposited nano-

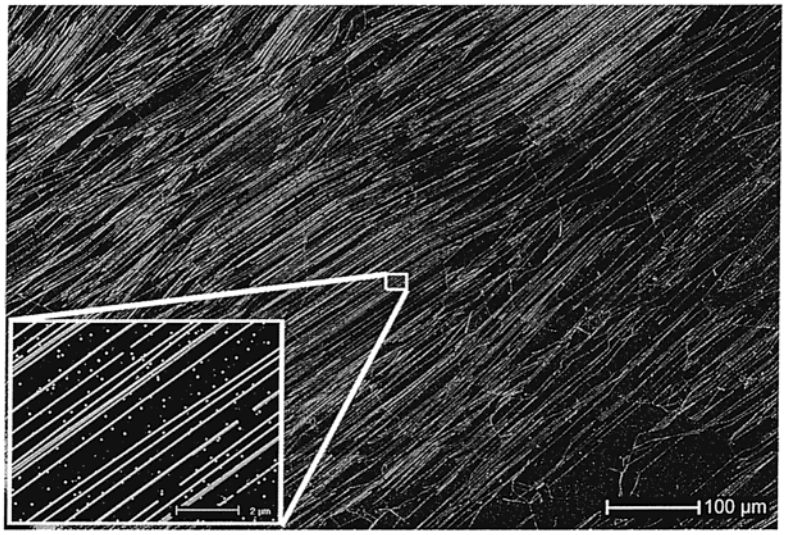

Figure 7. SEM image of an HOPG surface after the deposition of MoO_2 nanowires. The step edges present within individual grains on the HOPG surface are oriented parallel to one another. Steps are separated from one another by terraces with widths of 50−500 nm on average.

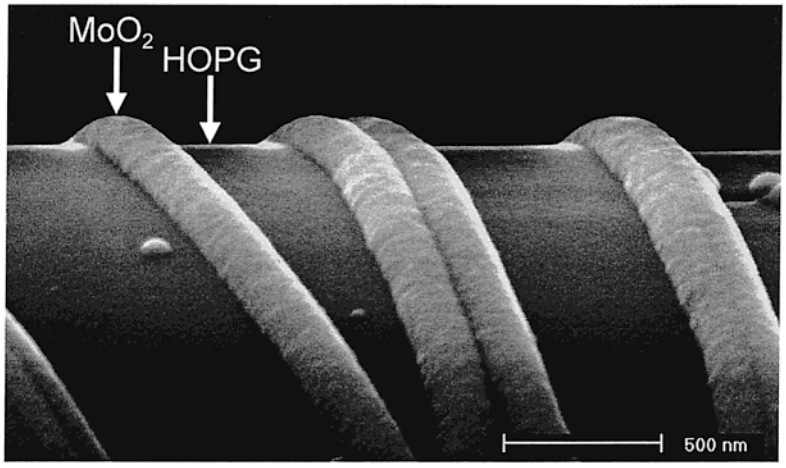

Figure 8. SEM image of MoO_2 nanowires traversing a curved graphite surface. This image conveys the uniformity and hemicylindrical profile of these wires.

wires such as those shown in Figure 11. Here is shown a freshly deposited MoO_2 nanowire before (left) and after (right) reduction at 500 °C for 1 h. Arrows indicate the diameter of three wires in each image. Before reduction, the diameter for all three wires was 570 nm; after reduction, the diameter is 460 nm, a shrinkage of 20%.

The completeness of the reduction is confirmed by electron diffraction (data not shown), X-ray fluorescence (data not shown), and XPS analysis of the nanowires (Figure 6B and Table 1). After reduction at 500−650 °C for 1 h, the Mo $3d_{5/2}$ binding energy was 228.1 eV, exactly the expected binding energy for molybdenum metal. In previous work[42] we have demonstrated that individual Mo^0 nanowires that are 300−400 nm in diameter exhibit a conductivity approximately an order of magnitude lower than molybdenum metal. The conductivity of nanowires in air, however, decreases as a function of time because of the growth, at the surface of the nanowire, of insulating MoO_3. The composition of this oxide was verified from XPS spectra of nanowires (Figure 6C) that were first reduced to Mo^0 and subsequently exposed to air for several weeks. The XPS spectrum of Figure 6C shows a positive shift in the energy of Mo $3d_{5/2}$ electrons from a value characteristic of Mo^0 (228.1 eV) to a value characteristic of MoO_3 (232.6 eV).

In contrast to MoO_2, Mo^0 nanowires are both resilient and resistant to breakage. Arrays of hundreds of Mo^0 nanowires may be embedded in a polymer film and lifted off of the graphite surface. For this purpose, we have found that some cyanoacrylates are excellent. Figure 12 shows the surface of two polystyrene films in which Mo^0 nanowires are embedded. In Figure 12A an uncoated polymer surface is shown together with a nanowire having a distinctive shape. This wire was released from the polymer film when it was flexed. Hemicylindrical tracks in this film, corresponding to the positions of individual nanowires on the graphite surface, are also clearly visible. Figure 12B shows a polymer surface with embedded Mo^0 nanowires. In this case, 5−10 nm of gold was evaporated onto the surface to eliminate charging effects. Using this technique, arrays of hundreds of long, dimensionally uniform metal nanowires can be lifted off the graphite surface. The ability to lift off parallel arrays of long nanowires is a general property of nanowires prepared by ESED on graphite.[56] This capability facili-

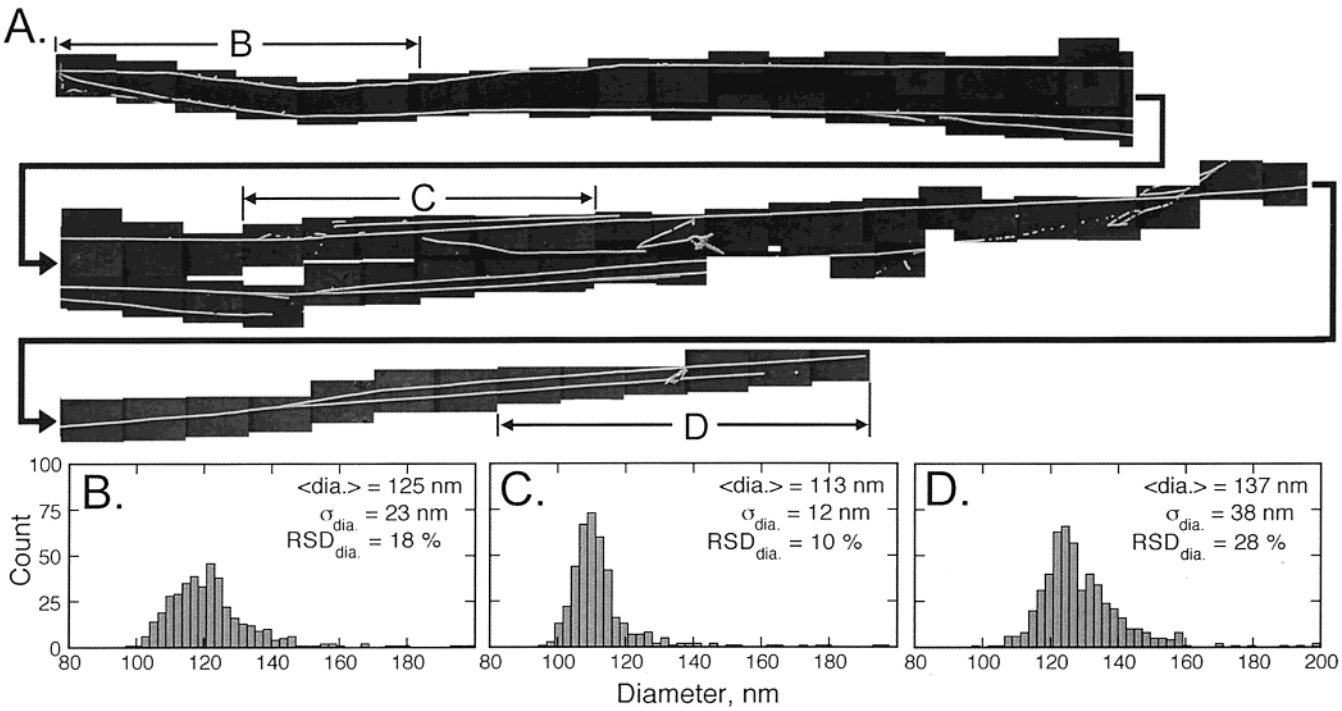

Figure 9. Statistical analysis of nanowire uniformity for a particular MoO_2 nanowire with a length of 147 μm. At the top (A) is shown a mosaic of 52 high-magnification SEM images. These images were used to compile 3500 measurements of the wire diameter along its axis to obtain a quantitative measure of its uniformity. The histograms (B−D) show the distribution of diameters in each region shown by the arrows labeled in part A.

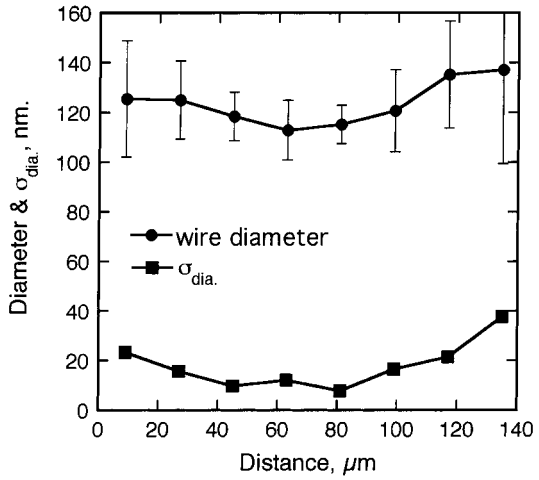

Figure 10. Pooled mean and standard deviations of the nanowire diameter measurements shown in Figure 9 plotted as a function of the axial position along the nanowire.

Scheme 2. Device for Monitoring the Resistance of Molybdenum Nanowire Arrays

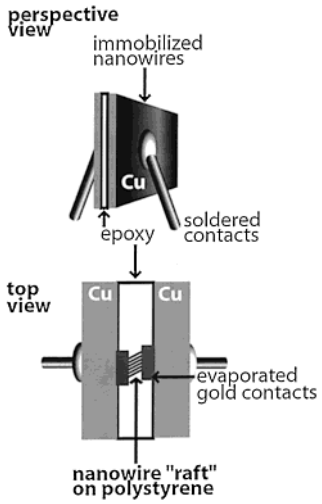

tates the incorporation of nanowire arrays into sensors[22,57] and electronic devices.

Because molybdenum nanowires that are exposed to air are gradually converted to MoO_3, these nanostructures cannot function indefinitely as conductors in oxidizing environments. We have measured the increase in resistance as a function of time for arrays of hundreds of 200−400 nm diameter wires using devices such as that shown in Scheme 2 (see the Experimental Section). Data for four such devices are shown in Figure 13. The rate of resistance increase for these four devices, measured over the course of a day, ranged from 1 to 2.5% h^{-1}. Also apparent in the data for three of these devices are abrupt, stepwise increases in the resistance of a few percent (arrows). Although the origin of these steps cannot be known with certainty, they may coincide with the disconnection of individual nanowires from the circuit caused either by breakage induced by the stress of oxidation or by failure of a gold contact. We have monitored the resistance of one nanowire array for more than 40 days. Over this period, its resistance increased by 23%. We conclude that, despite the susceptibility of Mo^0 nanowires to oxidation, this process takes place slowly over many weeks. These results suggest that it is reasonable to expect Mo^0 nanowires with diameters in the range from 200 to 400 nm to retain the ability to function as electrical conduits for months.

(56) Penner, R. M. *J. Phys. Chem. B* **2002**, *106*, 3339.
(57) Walter, E. C.; Favier, F.; Penner, R. M. *Anal. Chem.* **2002**, *74*, 1546.

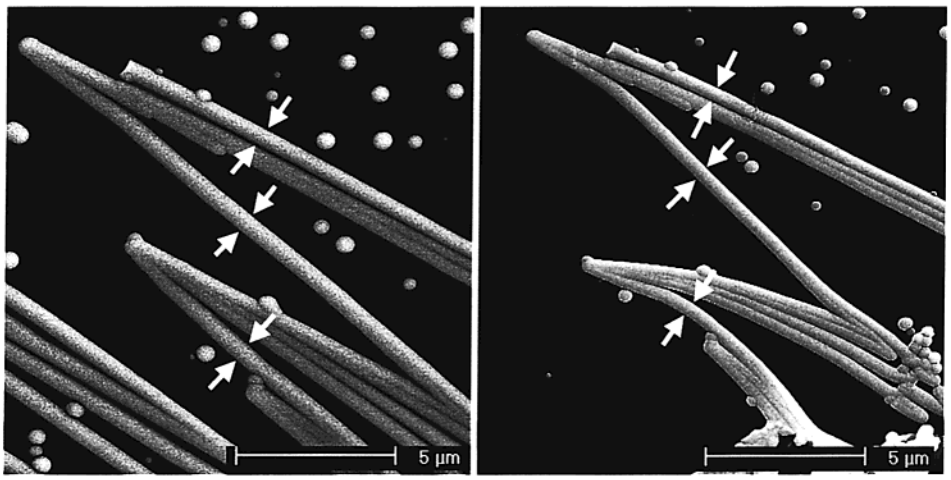

Figure 11. SEM micrographs of electrodeposited nanowires before (left) and after (right) reduction at 500 °C for 1 h. Arrows indicate the diameter of three wires in each image. Before reduction, this diameter for all three wires was 570 nm; after reduction, the diameter was 460 nm. This shrinkage is due to the difference in molar unit volume per Mo atom between MoO_2 and Mo^0.

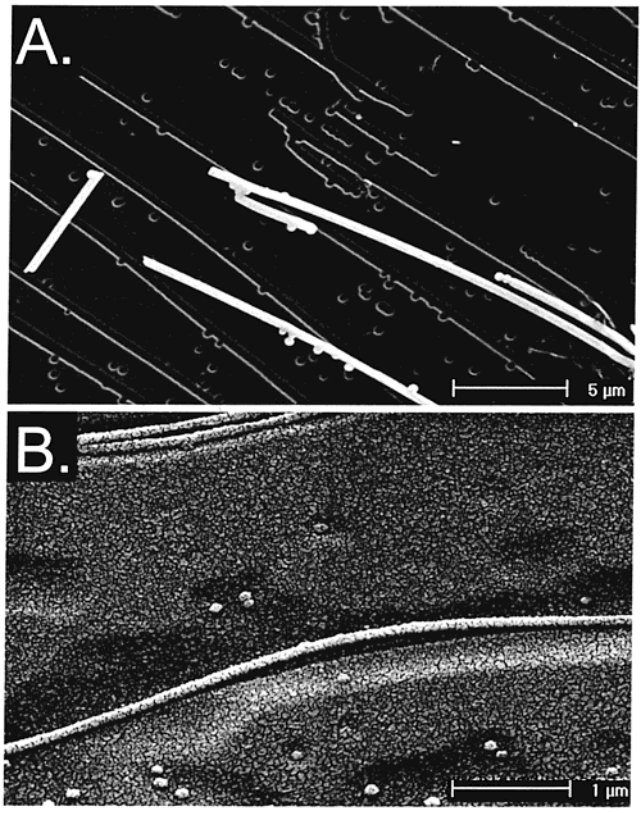

Figure 12. SEM images of the wires removed from the HOPG using polystyrene as the embedding and lift-off material. (A) Free-standing metallic Mo^0 wires after release from the polystyrene film. Note the wire (bright) with a shape identical with that of the polystyrene replica next to it (dark). The lower image shows supported metallic nanowires. The textured appearance seen in this image is caused by the presence of an evaporated gold film used to reduce charging effects in the SEM.

IV. Summary

Molybdenum nanowires that are up to 500 μm in length and 13 nm to 1.0 μm in diameter have been prepared by a two-step process involving the selective electrodeposition of MoO_2 at step edges on a graphite electrode surface, followed by reduction of these oxide nanowires to molybdenum metal at 500 °C in hydrogen.

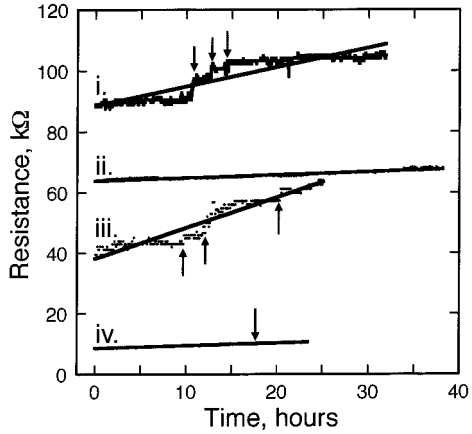

Figure 13. Resistance of four molybdenum nanowire arrays (cf. Scheme 2) plotted as a function of the duration of exposure to a laboratory air ambient (relative humidity ≈ 50%, $T \approx 22$ °C). The mean nanowire diameter in each array was 200−300 nm. The slopes of these lines varied from 1% h^{-1} (device iv) to 2.5% h^{-1} (device iii). XPS spectra (see Figure 6) reveal that this increase in resistance coincides with the formation of an insulating MoO_3 coating on each nanowire. Also indicated by arrows are the locations of abrupt increases in the resistance of these nanowire arrays. We attribute these resistance "steps" to the disconnection from the circuit of one or more nanowires caused by the progressive buildup of strain associated with the formation of a MoO_3 oxide on the surfaces of the nanowires.

The organization of nanowires on the graphite surface is dictated by the organization of step edges: Nanowires were organized into parallel arrays containing hundreds of individual wires separated from one another by 5−10 μm.

During growth, a time-independent deposition current was observed. This constant current leads to a growth law in which the diameter of MoO_2 nanowires increased in direct proportion to the square root of the deposition time. This growth law, which is identical in its time dependence to the diffusion-controlled growth law for spherical colloidal particles, may be the reason that MoO_2 nanowires become smooth during electrodeposition.

The reduction of MoO_2 nanowires at 500 °C for 1 h or more produced molybdenum metal nanowires. As com-

pared with MoO_2, molybdenum wires possessed better strength and resiliency. These nanowires could be lifted off of the graphite surface intact by embedding them in a polymer or epoxy film. Molybdenum metal oxidizes in air to produce insulating MoO_3; however, for nanowires that are several hundred nanometers in diameter, this process occurs slowly over the course of several weeks at a rate of $1-2\%\ day^{-1}$, on average.

We have verified that the two-step procedure outlined in this paper can be used to obtain nanowires for other metals including copper and iron. A clear requirement is that an electronically conductive oxide of the metal in question can be electrodeposited. In the cases of copper and iron, these oxides appear to be Cu_2O and Fe_2O_3. The only metals that are clearly excluded by this requirement are the noble metals for which stable, conductive oxides are not thermodynamically accessible.

Acknowledgment. This work was funded by the NSF (Grant CHE 0111557) and the Petroleum Research Fund of the American Chemical Society (33751-AC5). K.I. and J.C.H. acknowledge funding support from the DOE (DE-FG03-96ER45576). We also gratefully acknowledge an American Chemical Society, Division of Analytical Chemistry, Fellowship, sponsored by Merck & Co., to M.P.Z. R.M.P. acknowledges the financial support of the A.P. Sloan Foundation Fellowship and the Camille and Henry Dreyfus Foundation. Finally, donations of graphite by Dr. Art Moore of Advanced Ceramics are gratefully acknowledged.

CM020249A